IEEE Conference on Decision and Control (CDC), Hawaii, USA, 2012

Leader-Follower Formation of Marine Craft using Constraint Forces and Lagrange Multipliers

Ehsan Peymani Thor I. Fossen

Abstract— **In this paper, we make a connection between formation control of underactuated marine craft and modeling of constrained multibody systems. We propose a dynamic controller for master-slave formations, which accomplishes the path-maneuvering task of the master and the synchronization of the leaders with the master. Computer simulations are also conducted for identical INFANTE AUVs to verify the validity of the theoretical developments. Robustness with respect to irrotational constant ocean currents is also studied.**

I. INTRODUCTION

There are many cases that show a formation of smaller and less complicated systems can outperform larger and more sophisticated ones. For instance, one can mention pipeline inspection and seabed mapping [1], in which a cooperative group of marine vehicles can lower the operation cost and time while enhancing the quality and reliability.

A considerable number of articles have been published in the field of coordinated and cooperative control of autonomous vehicles; [2]–[4] provide a fresh and profound insight into the topic. Roughly speaking, one can categorize them into leader-follower, behavior-based, and virtual structure methods. Techniques based on graph-theory and artificial potentials are also available.

For high-speed maritime applications, formation control of *underactuated* marine craft (UMC) takes precedence. In [5], a cross-track formation controller for UMC is designed so that the formation moves along a straight-line path while the members are aware of the path and the desired speed. Utilizing Lyapunov-based techniques and the graph theory, [1] designs a formation controller for UMC which is robust to communication failures. For the leader-follower scheme, sliding model control laws are derived for a fleet of UMC in [6]. Dong and Farrell [7] propose a controller for UMC to converge to stationary formation patterns with a desired orientation. Some of the seminal works for multiple fully actuated marine vehicles are [8]–[10]. In contrast to the above-mentioned articles, in this paper, we take advantage of physical information subtly hidden behind the equations of motion, and seek forces that UMC would exert on one another if they were connected physically.

The main contribution of this paper is to portray the formation control problem as a constrained multibody system, and exploit the explicit structure of the Lagrangian formulation so as to design a controller according to first principles by virtue of Lagrangian mechanics and the concept of constraint forces. The strength of the proposed strategy lies in simplicity, physical interpretation, and applicability to groups of any number of vehicles. The control method provides control inputs for both the leader and the followers simultaneously such that the leader follows the desired path with the commanded speed and the followers establish the desired geometric configuration and retain it. The paper deals with underactuated marine craft, and can be viewed as an extension to [11] where positional constraints and fully actuated marine craft are taken into consideration.

The outline of the paper is as follows. In Section II, the problem is clearly stated. After that, the concept of virtually constrained motion controllers is set out. The master-slave formation control problem is then characterized as constrained multibody systems in Section IV where formation modeling and the constraints that are imposed on the system are explained. Then, the formation control forces are derived. At the end, the designed control system is evaluated for a nonlinear model of INFANTE.

II. PROBLEM STATEMENT

In this paper, we study the problem of formation control for a group of underactuated surface marine craft. Without loss of generality, we focus on a group of two craft. A common example can be underway replenishment operation [12], where one marine craft plays the role of master and the other, called slave, has to maintain its position relative to the master while the master follows the desired path with the desired speed profile. Therefore, the problem can be decomposed into two tasks:

1) *Path maneuvering* of the master in which the master follows the path while it retains the speed as desired.
2) *Synchronization* of the slave with the master such that the desired formation is achieved.

The objective is to propose a method that designs a decentralized controller to accomplish these two tasks for a group of two marine craft under Assumption 1.

Assumption 1: The following assumptions are made:

- Each marine craft has access to its own pose and velocities.
- The slave receives the information about the master's position and velocities through a flawless communication channel. The slave has no knowledge about the desired speed and the path that the master has to follow.
- The desired path to be followed by the master is feasible, known, and smooth.

Peymani is with the Center for Ships and Ocean Structures; Peymani and Fossen are with the Department of Engineering Cybernetics, Norwegian University of Science & Technology, Trondheim, Norway. ehsan@ntnu.no and fossen@ieee.org.

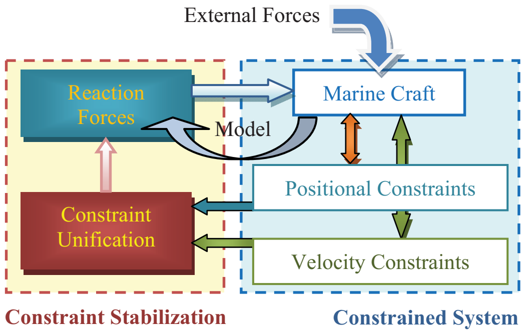

Fig. 1: Schematic diagram of the virtually constrained motion control scheme

III. Control Methodology

The control method that is proposed in this paper is based on Lagrangian mechanics. The formation control problem for a group of mechanical systems can be regarded as modeling of a multibody system, connected by means of physical elements such as rods, springs, and dampers. In multibody systems, connections between the bodies restrict the position and velocity of the bodies, and it turns out that the bodies exert forces on each other via the connecting elements. One way to describe the motion of multibody mechanical systems subject to inter-body constraints is to employ the Lagrange multiplier method. This idea is taken into account to derive a control law that achieves the desired formation patterns.

In fact, in the proposed technique, each marine craft is considered as a body which is constrained by its neighbors such that the desired geometric configuration is obtained. That is, the constraints are imposed on the bodies by virtue of control objectives and they are not physically present. They are called *virtual constraints*. The goal is to find the forces that these virtual constraints exert on each body in order to make and preserve the configuration. Then, the constraint forces are applied to each vehicle by means of its actuators.

Figure 1 captures a schematic diagram of the proposed method, termed *virtually constrained motion control scheme*. It is seen that the technique includes formation modeling and control. First, we explain the modeling block by a brief review of the facts from Lagrangian mechanics; then, we set out how the constraint forces are derived so that the constraints always hold.

A. Lagrangian Mechanics for Constrained Motion

A large group of unconstrained mechanical systems can be represented by the following equation [13]:

$$\mathcal{M}(\boldsymbol{q})\ddot{\boldsymbol{q}} = \boldsymbol{F}(\boldsymbol{q}, \dot{\boldsymbol{q}}, t) \tag{1}$$

where $\boldsymbol{q} \in \mathbb{R}^n$ is a vector of generalized coordinates that uniquely characterizes the position and orientation of the system in an n-dimensional configuration space. n is the number of degrees of freedom (DOF). The time-derivative of $\boldsymbol{q}$, denoted $\dot{\boldsymbol{q}}$, is called the generalized velocity vector. $\mathcal{M}(\boldsymbol{q}) = \mathcal{M}^{\mathrm{T}}(\boldsymbol{q}) \in \mathbb{R}^{n\times n}, \mathcal{M}(\boldsymbol{q}) > 0$ is the mass and inertia matrix. We may have $\boldsymbol{F}(\boldsymbol{q}, \dot{\boldsymbol{q}}, t) = \boldsymbol{\tau} - \boldsymbol{n}(\boldsymbol{q}, \dot{\boldsymbol{q}})$ where $\boldsymbol{n}(\boldsymbol{q}, \dot{\boldsymbol{q}})$ includes Coriolis-centripetal, potential and viscous forces, and $\boldsymbol{\tau} \in \mathbb{R}^n$ is the vector of generalized forces, arising from actuators or external disturbances.

Constrained Motion: The motion of a system might be restricted to assorted constraints classified under various criteria. This paper focuses on equality constraints. *Holonomic constraints* are those which are expressed in terms of generalized coordinates, i.e. $g(\boldsymbol{q}, t) = 0$. Constraints involving generalized velocities are said to be *kinematic constraints* [14], i.e. $k(\boldsymbol{q}, \dot{\boldsymbol{q}}, t) = 0$. When the system is subject to l holonomic and m kinematic constraints, the constraint functions are represented as

$$\boldsymbol{G}(\boldsymbol{q}, t) = 0_l \qquad l < n \tag{2}$$

$$\boldsymbol{K}(\boldsymbol{q}, \dot{\boldsymbol{q}}, t) = 0_m \qquad m \leq n \tag{3}$$

where 0_i is the i-vector of zeros and t is the time variable. A frequently used form of (3) is linear in velocity:

$$\boldsymbol{K}(\boldsymbol{q}, \dot{\boldsymbol{q}}, t) \triangleq \mathcal{A}(\boldsymbol{q}, t)\dot{\boldsymbol{q}} + \boldsymbol{b}(\boldsymbol{q}, t) \tag{4}$$

in which $\mathcal{A} \in \mathbb{R}^{m\times n}, \boldsymbol{b} \in \mathbb{R}^m$. Kinematic constraints (3) are intrinsically holonomic if they are integrable. Otherwise, they are called *nonholonomic*. The linear-in-velocity kinematic constraints (4) are termed *Pfaffian* if they are driftless and stationary. Refer to [13] for more details.

The Force of Constraints: The most popular approach to deal with constrained motion employs the Lagrange multiplier method. Actually, this approach assumes that constraints exert additional forces on the system; thus, the equations of motion have to be rectified.

Utilizing a generalization of D'Alembert's principle and introducing a vector of multipliers $\boldsymbol{\lambda}_G \in \mathbb{R}^l$, the force of holonomic constraints follows from (e.g. see [15])

$$\boldsymbol{\tau}_G = -\mathcal{W}_G^{\mathrm{T}}(\boldsymbol{q}, t)\boldsymbol{\lambda}_G, \qquad \mathcal{W}_G = \partial \boldsymbol{G}/\partial \boldsymbol{q} \in \mathbb{R}^{l\times n} \tag{5}$$

The approach does not arrive at a conclusive result for the force of general nonholonomic constraints [16]. Nonetheless, if nonholonomic constraints are restricted to those which are linear in velocity variables, i.e. of the form (4), the principle of D'Alembert is applicable and the reaction force is given by

$$\boldsymbol{\tau}_K = -\mathcal{A}^{\mathrm{T}}(\boldsymbol{q}, t)\boldsymbol{\lambda}_K, \quad \boldsymbol{\lambda}_K \in \mathbb{R}^m \tag{6}$$

To sum up, if a system is subject to l holonomic and m nonholonomic functions, the overall force of constraints is

$$\boldsymbol{\tau}_c = \boldsymbol{\tau}_G + \boldsymbol{\tau}_K \tag{7}$$

which is superimposed onto the model of the system as though the system can move freely in the configuration space but it is under the influence of some additional forces. Thus, the equations of motion (1) are rectified as:

$$\mathcal{M}(\boldsymbol{q})\ddot{\boldsymbol{q}} = \boldsymbol{F}(\boldsymbol{q}, \dot{\boldsymbol{q}}, t) + \boldsymbol{\tau}_c \tag{8}$$

It is now possible to recast the overall constraint force (7) as

$$\boldsymbol{\tau}_c = -\mathcal{W}^{\mathrm{T}}\boldsymbol{\lambda} \tag{9}$$

where $\boldsymbol{\lambda} \triangleq [\boldsymbol{\lambda}_K^{\mathrm{T}}, \boldsymbol{\lambda}_G^{\mathrm{T}}]^{\mathrm{T}} \in \mathbb{R}^{l+m}$ is the multiplier vector and $\mathcal{W} \triangleq [\mathcal{A}^{\mathrm{T}}, \mathcal{W}_G^{\mathrm{T}}]^{\mathrm{T}} \in \mathbb{R}^{(m+l)\times n}$ is the constraint Jacobian matrix.

B. Constraint Stabilization

This section is dedicated to the Constraint Stabilization block in Fig. 1. The aim of the constraint stabilization is to assure that the constraints are always satisfied and if they are violated, for instance, due to inconsistent initial conditions or external disturbances, they are properly enforced. A two-step procedure is presented for stabilization. In the first step, holonomic functions are stabilized at the velocity level in order to be merged with nonholonomic constraints; a unified constraint function is then defined. In the next step, the unified function is stabilized and the vector of reaction forces is derived. We now clarify the stabilization procedure.

Step 1: "Constraint Unification" aims to make the manifold corresponding to the holonomic constraints (2) attractive and invariant using $\dot{\boldsymbol{G}} = \boldsymbol{u}_{2G}$. Selecting $\boldsymbol{u}_{2G} = -\mathcal{P}_G\boldsymbol{G}$, where $\mathcal{P}_G \in \mathbb{R}^{l\times l}$ is positive definite, makes $\boldsymbol{G} = 0_l$ globally exponentially stable (GES). Denoting $\boldsymbol{G}^t = \partial\boldsymbol{G}/\partial t \in \mathbb{R}^l$, it gives rise to

$$\dot{\boldsymbol{G}} + \mathcal{P}_G\boldsymbol{G} = 0_l \Rightarrow \mathcal{W}_G\dot{\boldsymbol{q}} + \boldsymbol{G}^t + \mathcal{P}_G\boldsymbol{G} = 0_l \qquad (10)$$

Since (10) and (4) are identical in structure, we lump them together and define a *unified constraint function* given by

$$\boldsymbol{\Phi}(\boldsymbol{q}, \dot{\boldsymbol{q}}, t) \triangleq \mathcal{W}(\boldsymbol{q}, t)\dot{\boldsymbol{q}} + \boldsymbol{a}(\boldsymbol{q}, t) \qquad (11)$$

$$\boldsymbol{a}(\boldsymbol{q}, t) = \begin{bmatrix} \boldsymbol{b}(\boldsymbol{q}, t) \\ \boldsymbol{G}^t(\boldsymbol{q}, t) + \mathcal{P}_G\boldsymbol{G}(\boldsymbol{q}, t) \end{bmatrix} \in \mathbb{R}^{l+m} \qquad (12)$$

Step 2: The unified function $\boldsymbol{\Phi}$ has to be always zero. Akin to Step 1, $\boldsymbol{\Phi} = 0_{l+m}$ is made globally exponentially stable. Considering $\dot{\boldsymbol{\Phi}} = \boldsymbol{u}_\Phi$ and picking $\boldsymbol{u}_\Phi = -\mathcal{P}_\Phi\boldsymbol{\Phi}$, where $\mathcal{P}_\Phi \in \mathbb{R}^{(l+m)\times(l+m)}$ is positive definite, it follows that

$$\dot{\boldsymbol{\Phi}} + \mathcal{P}_\Phi\boldsymbol{\Phi} = 0_{l+m} \Rightarrow \mathcal{W}\ddot{\boldsymbol{q}} + \dot{\mathcal{W}}\dot{\boldsymbol{q}} + \dot{\boldsymbol{a}} + \mathcal{P}_\Phi\boldsymbol{\Phi} = 0_{l+m} \quad (13)$$

Reaction Forces: To derive the force of constraints, one requires to solve the equation of motion (8) for acceleration:

$$\ddot{\boldsymbol{q}} = \mathcal{M}(\boldsymbol{q})^{-1}\left(\boldsymbol{F}(\boldsymbol{q}, \dot{\boldsymbol{q}}, t) + \boldsymbol{\tau}_c\right) \qquad (14)$$

Equation (14) is substituted in (13), and it yields the following equation for the multiplier vector

$$\mathcal{W}\mathcal{M}^{-1}\mathcal{W}^{\mathrm{T}}\boldsymbol{\lambda} = \mathcal{W}\mathcal{M}^{-1}\boldsymbol{F} + \dot{\mathcal{W}}\dot{\boldsymbol{q}} + \dot{\boldsymbol{a}} + \mathcal{P}_\Phi\boldsymbol{\Phi} \qquad (15)$$

In (15), if $\mathcal{W}$ is full row rank, the product $\mathcal{W}\mathcal{M}^{-1}\mathcal{W}^T$ is a nonsingular square matrix since $\mathcal{M}$ is nonsingular. After computing the vector of multipliers $\boldsymbol{\lambda}$, the reaction forces are found using (9) at each instant of time. In case $m + l > n$ but $\mathcal{W}$ has n linearly independent columns, the product $\mathcal{W}\mathcal{M}^{-1}\mathcal{W}^{\mathrm{T}}$ is not invertible. To solve this problem, the constraint force vector can be directly computed from (15) by utilizing the Moore-Penrose (MP) pseudo-inverse for $\mathcal{W}\mathcal{M}^{-1}$. Since $\mathcal{W}\mathcal{M}^{-1}$ is full column rank, its MP pseudo-inverse, denoted $(\mathcal{W}\mathcal{M}^{-1})^\dagger$, is equal to $\mathcal{M}\mathcal{W}^\dagger$ in which $\mathcal{W}^\dagger = (\mathcal{W}^{\mathrm{T}}\mathcal{W})^{-1}\mathcal{W}^{\mathrm{T}}$. Consequently, the vector of constraint forces emerges as

$$\boldsymbol{\tau}_c = -\boldsymbol{F}(\boldsymbol{q}, \dot{\boldsymbol{q}}, t) - \mathcal{M}\mathcal{W}^\dagger\left(\dot{\mathcal{W}}\dot{\boldsymbol{q}} + \dot{\boldsymbol{a}} + \mathcal{P}_\Phi\boldsymbol{\Phi}\right) \qquad (16)$$

In this case, the control law is computed such that $\|\mathcal{W}\mathcal{M}^{-1}\boldsymbol{\tau}_c + Y\|^2$, where Y is the right-hand side of (15), is minimized.

Notice that inconsistent constraints must be avoided. Those constraints that conflict one another are said to be inconsistent or conflicting. Moreover, it is required that the constraints are independent, meaning that they are not redundant or unnecessary.

Remark 1: The derived control laws (15) and (16) follow from first principles and are physically interpretable. One can consider that viewing control objectives as virtual constraints along with a stabilization process resembles placing generalized dampers and springs between bodies. Violation of constraints is tantamount to the fact that dampers and springs leave their equilibrium, and consequently they exert forces on the bodies.

Remark 2: It is worth mentioning that there exist many choices for $\boldsymbol{u}_G$ and $\boldsymbol{u}_\Phi$, and they can be found such that the overall system becomes robust with respect to uncertainties and external disturbances.

Remark 3: It is discernible that the proposed stabilization approach bears superficial resemblance to the recursive method of backstepping [17] and the sliding-mode control strategy [18]. Also notice that for positional constraints proportional-derivative (PD-type) controllers are designed while velocity constraints are stabilized by proportional (P-type) controllers.

IV. Formation Control Problem

In this section, the problem of master-slave formation of two marine craft is portrayed as modeling of constrained multibody systems. First, we present the typical model for marine craft according to [19]; then the control objectives are expressed in terms of the constraints that are placed on the system.

A. 3-DOF Model of Marine Craft

1) Individual Vehicle: Consider the vehicle pose $\boldsymbol{q} = [\boldsymbol{p}^{\mathrm{T}}, \psi]^{\mathrm{T}}$ where $\boldsymbol{p} = [x, y]^{\mathrm{T}} \in \mathbb{R}^2$ and $\psi \in \mathcal{S}$ is the yaw angle; $\boldsymbol{\nu} = [u, v, r]^{\mathrm{T}} \in \mathbb{R}^3$, where u and v are the linear velocities and r is the angular velocity expressed in the body-fixed reference frame $\{b\}$. Let $\mathcal{J}(\psi) = \mathrm{diag}\{\mathcal{R}(\psi), 1\}$ be the rotation matrix from $\{b\}$ to the inertial reference frame, represented by $\{i\}$. The matrix $\mathcal{R}(\psi)$ is given by

$$\mathcal{R}(\psi) = \begin{bmatrix} \cos(\psi) & -\sin(\psi) \\ \sin(\psi) & \cos(\psi) \end{bmatrix} \in \mathcal{SO}(2) \qquad (17)$$

$$\dot{\mathcal{R}}(\psi) = \mathcal{R}(\psi)\mathcal{S}(\psi) \qquad \mathcal{S}(\psi) = \begin{bmatrix} 0 & -1 \\ 1 & 0 \end{bmatrix}\dot{\psi} \qquad (18)$$

According to [19], the dynamic equations are described by

$$\dot{\boldsymbol{q}} = \mathcal{J}(\psi)\boldsymbol{\nu} \qquad (19a)$$

$$\mathcal{M}_b\dot{\boldsymbol{\nu}} + \mathcal{C}_b(\boldsymbol{\nu})\boldsymbol{\nu} + \mathcal{D}_b(\boldsymbol{\nu})\boldsymbol{\nu} = \boldsymbol{\tau}_b \qquad (19b)$$

in which $\mathcal{M}_b = \mathcal{M}_b^{\mathrm{T}} > 0$, $\dot{\mathcal{M}}_b = 0$, $\mathcal{C}_b = -\mathcal{C}_b^{\mathrm{T}}$, and $\mathcal{D}_b > 0$. Homogeneous mass distribution and xz-plane symmetry are presumed, and the surge dynamics is assumed to be decoupled from the sway-yaw dynamics; thus, the system matrices take the forms

$$\mathcal{M}_b = \begin{bmatrix} m_{11} & 0 & 0 \\ 0 & m_{22} & m_{23} \\ 0 & m_{23} & m_{33} \end{bmatrix}, \quad \mathcal{D}_b = \begin{bmatrix} d_{11} & 0 & 0 \\ 0 & d_{22} & d_{23} \\ 0 & d_{23} & d_{33} \end{bmatrix} \tag{19c}$$

$$\mathcal{C}_b = \begin{bmatrix} 0 & 0 & -(m_{22}v + m_{23}r) \\ 0 & 0 & m_{11}u \\ (m_{22}v + m_{23}r) & -m_{11}u & 0 \end{bmatrix} \tag{19d}$$

where linear damping is assumed. Extension to encompass nonlinear damping forces is possible but this is outside the scope of this paper. In (19b), $\boldsymbol{\tau}_b \triangleq [\tau_u, \tau_v, \tau_r]^{\mathrm{T}}$ represents the vector of generalized forces acting on the system expressed in $\{b\}$ and captures forces and moments due to actuators as well as due to external disturbances. τ_u is a function of the forward thrust, denoted T, and τ_r depends on the rudder deflection, denoted δ. Underactuated marine craft lack an independent actuator for sway dynamics. We assume $\tau_v = 0$.

Utilizing (19a), the kinetics (19b) is translated into the form (8) where $\mathcal{M}(\boldsymbol{q}) = \mathcal{J}(\psi)\mathcal{M}_b\mathcal{J}^{\mathrm{T}}(\psi)$, $\boldsymbol{\tau} = \mathcal{J}(\psi)\boldsymbol{\tau}_b^p$ and $\boldsymbol{n}(\boldsymbol{q}, \dot{\boldsymbol{q}}) = \mathcal{C}_n(\boldsymbol{q}, \dot{\boldsymbol{q}})\dot{\boldsymbol{q}} + \mathcal{D}_n(\boldsymbol{q}, \dot{\boldsymbol{q}})\dot{\boldsymbol{q}}$ in which $\mathcal{C}_n$ and $\mathcal{D}_n$ can be found by inspection.

2) A Group of Vehicles: For a fleet of marine vehicles, each vehicle together with corresponding signals and matrices is indexed by j; that is, $\mathcal{M}_j(\boldsymbol{q}_j)\ddot{\boldsymbol{q}}_j = \boldsymbol{F}_j(\boldsymbol{q}_j, \dot{\boldsymbol{q}}_j, t)$ for $j = \{m, s\}$ represents the model of the master vehicle and the slave vehicle, respectively. The vector of generalized coordinates is formed by stacking $\boldsymbol{q}_m$ and $\boldsymbol{q}_s$ (i.e. $\boldsymbol{q} = [\boldsymbol{q}_m^{\mathrm{T}}, \boldsymbol{q}_s^{\mathrm{T}}]^{\mathrm{T}}$). Consequently, the formation is described by (8) where

$$\mathcal{M}(\boldsymbol{q}) = \mathrm{diag}\{\mathcal{M}_m(\boldsymbol{q}_m), \mathcal{M}_s(\boldsymbol{q}_s)\} \tag{21}$$

$$\boldsymbol{F}(\boldsymbol{q}, \dot{\boldsymbol{q}}, t) = [\boldsymbol{F}_m^{\mathrm{T}}(\boldsymbol{q}_m, \dot{\boldsymbol{q}}_m, t), \boldsymbol{F}_s^{\mathrm{T}}(\boldsymbol{q}_s, \dot{\boldsymbol{q}}_s, t)]^{\mathrm{T}} \tag{22}$$

$$\boldsymbol{\tau}_c = [\boldsymbol{\tau}_{c,m}^{\mathrm{T}}, \boldsymbol{\tau}_{c,s}^{\mathrm{T}}]^{\mathrm{T}} \tag{23}$$

B. Virtual Constraints

Now, we lay out the constraints that are imposed on the multibody system due to the control objectives. As mentioned in section II, the formation control problem is divided into two tasks. One is carried out by the leader, and the other is conducted by the follower.

1) Constraints on the Leader: The leader must follow the parameterized path with the desired speed profile, $u_d(t) > 0, \forall t > 0$. The position of each point on the path is denoted $\boldsymbol{p}_p(\varrho) = [x_p(\varrho), y_p(\varrho)]^{\mathrm{T}} \in \mathbb{R}^2, \varrho \in \mathbb{R}$. Consider a virtual vehicle (VV) moving along the path. Thus, the position of the VV takes that of the path and is denoted $\boldsymbol{p}_p(\varpi), \varpi \in \mathbb{R}$. The VV's heading angle is equal to the slope of the path tangential line, which is computed by $\psi_p = \arctan(y_p^{'}/x_p^{'})$ where $x^{'}(\varrho) \triangleq \frac{\partial x}{\partial \varrho}$, $\psi_p \in [-\pi, \pi]$. The body-fixed reference frame of VV is denoted $\{p\}$. $\boldsymbol{v}_p = [u_p, 0]^{\mathrm{T}}$ represents the linear velocity of VV expressed in $\{p\}$. As the VV's speed is u_p, the following update law is obtained

$$\dot{\varpi} = \frac{u_p}{\sqrt{(x_p^{'})^2 + (y_p^{'})^2}} \tag{24}$$

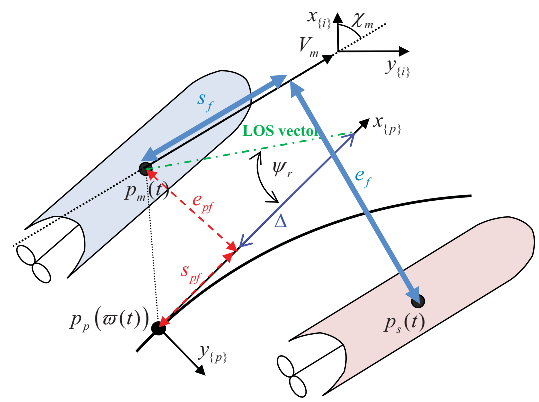

Fig. 2: The geometry of master-slave formation of two surface marine craft.

The error vector between the leader and the VV, expressed in $\{p\}$, is denoted $\boldsymbol{\varepsilon}_{pf} \triangleq [s_{pf}, e_{pf}]^{\mathrm{T}}$ and given by

$$\boldsymbol{\varepsilon}_{pf} = \mathcal{R}^{\mathrm{T}}(\psi_p)\left(\boldsymbol{p}_m - \boldsymbol{p}_p\right) \tag{25}$$

where s_{pf} is the along-track error and e_{pf} is the cross-track error. Fig. 2 captures the geometry of the problem in hand.

From the standpoint of constrained multibody systems, the path maneuvering problem [20] for the leader is equivalent to restricting the motion of the leader to that of the VV so that the leader follows the path in the desired direction with the commanded speed. Therefore, the following five constraints are placed on the leader:

$$\boldsymbol{K}_m \triangleq \mathcal{R}^{\mathrm{T}}(\psi_m)\dot{\boldsymbol{p}}_m - [u_d, v_{d,m}]^{\mathrm{T}} \tag{26}$$

$$\boldsymbol{G}_m \triangleq \left[G_{m,1}, \boldsymbol{\varepsilon}_{pf}^{\mathrm{T}}\right]^{\mathrm{T}}, \quad G_{m,1} \triangleq \psi_m - \psi_d \tag{27}$$

The nonholonomic constraints $\boldsymbol{K}_m$ are placed on u_m and v_m. The reader might wonder why a constraint is put on the sway dynamics while it is unactuated and what $v_{d,m}$ is. Let us gloss over the reasoning behind choosing this constraint and only mention that the constraint is neither conflicting nor redundant. It will be discussed in the next section. The holonomic constraints are imposed on $\boldsymbol{\varepsilon}_{pf}$ and the heading. ψ_d is recognized as the desired heading. The leader is asked to follow the desired heading angle so that it reaches the path as smoothly as desired. Inspired by the line-of-sight guidance method for straight-line path following [21], the desired heading is computed using (see Fig. 2)

$$\psi_d = \psi_p + \psi_r, \qquad \psi_r = \arctan(-\frac{e_{pf}}{\Delta}), \quad \Delta > 0 \tag{28}$$

where the relative angle $\psi_r \in [-\pi/2, \pi/2]$. The speed of the VV, u_p, has not been assigned yet. One choice may be $u_p = u_d$. However, it is recommended to use $u_p = u_d + \sigma s_{pf}$, $\sigma > 0$ since this choice makes the VV speed up, slow down, or even move backward so that it can stay at the shortest distance to the leader; accordingly, it reduces the leader's control effort and improves the performance.

2) Constraints on the Follower: The follower has to synchronize itself with the leader such that the desired geometric configuration is made. Therefore, we place the following three constraints on the follower:

$$\boldsymbol{K}_s \triangleq \mathcal{R}^{\mathrm{T}}(\psi_s)\dot{\boldsymbol{p}}_s - [u_m, v_{d,s}]^{\mathrm{T}} \tag{29}$$

$$G_{s,1} \triangleq \psi_s - \psi_m \tag{30}$$

The nonholonomic constraints place restrictions on the velocity components of the slave; The first constraint forces the slave to asymptotically track the forward velocity of the master. The second constraint function is put on the unactuated sway dynamics and $v_{d,s}$ is not assigned arbitrarily. It is demonstrated in the next section that $v_{d,s}$ must be adjusted according to the dynamics of the system and the controller. The holonomic constraint $G_{s,1}$ indicates that the follower has to own the leader's orientation.

The follower must remain in the desired position relative to the leader while it does not have knowledge about the leader's path; thus, the path has to be estimated. One way to estimate the leader's path is to conceive that the path is composed of straight-line segments. Let $\boldsymbol{\varepsilon}_f \triangleq [s_f, e_f]^{\mathrm{T}}$ denote the distance between the follower and a point on the estimated path, represented by $\boldsymbol{p}^*$, such that:

$$\boldsymbol{\varepsilon}_f = \mathcal{R}^{\mathrm{T}}(\psi^*)\,(\boldsymbol{p}_s - \boldsymbol{p}^*) \tag{31}$$

in which ψ^* is the slope of the estimated path. If $\boldsymbol{\varepsilon}_d = [s_d, e_d]^{\mathrm{T}}$ describes the desired formation, the following holonomic constraints are imposed on the follower:

$$\boldsymbol{G}_{s,2} \triangleq \boldsymbol{\varepsilon}_f - \boldsymbol{\varepsilon}_d \tag{32}$$

Thus, $\boldsymbol{G}_s = [G_{s,1}, \boldsymbol{G}_{s,2}^{\mathrm{T}}]^{\mathrm{T}}$. Consequently, the multibody system is subject to 10 constraints expressed in (26), (27), (29), (30), and (32).

V. The Control Law

To derive the force of constraints (23), the aforementioned stabilization procedure resulting in (15) and equivalently (16) is utilized. What is required is to form the constraint Jacobian matrix $\mathcal{W}$, and examine its rank property. To that end, the time derivatives of $\boldsymbol{\varepsilon}_{pf}$ and $\boldsymbol{\varepsilon}_f$ are computed and given by:

$$\dot{\boldsymbol{\varepsilon}}_{pf} = \mathcal{R}(\psi_p)^{\mathrm{T}}\dot{\boldsymbol{p}}_m + \mathcal{S}(\psi_p)^{\mathrm{T}}\boldsymbol{\varepsilon}_{pf} - \boldsymbol{\upsilon}_p$$
$$\dot{\boldsymbol{\varepsilon}}_f = \mathcal{R}(\psi^*)^{\mathrm{T}}\dot{\boldsymbol{p}}_s + \mathcal{S}(\psi^*)^{\mathrm{T}}\boldsymbol{\varepsilon}_f - \mathcal{R}(\psi^*)^{\mathrm{T}}\dot{\boldsymbol{p}}^*$$

Therefore, one can write the constraint Jacobian matrix for each vehicle as:

$$\mathcal{W}_m = \begin{bmatrix} \mathcal{R}^{\mathrm{T}}(\psi_m) & 0_{2,1} & 0_{2,3} \\ 0_{1,2} & 1 & 0_{1,3} \\ \mathcal{R}^{\mathrm{T}}(\psi_p) & 0_{2,1} & 0_{2,3} \end{bmatrix}$$
$$\mathcal{W}_s = \begin{bmatrix} \bar{\mathcal{W}}_s & \mathcal{R}^{\mathrm{T}}(\psi_s) & 0_{2,1} \\ \bar{w}_s & 0_{1,2} & 1 \\ 0_{2,3} & \mathcal{R}^{\mathrm{T}}(\psi^*) & 0_{2,1} \end{bmatrix}$$

where $0_{i,j}$ denotes an $i \times j$ zero matrix, and

$$\bar{\mathcal{W}}_s = \begin{bmatrix} -\cos(\psi_m) & -\sin(\psi_m) & 0 \\ 0 & 0 & 0 \end{bmatrix}$$
$$\bar{w}_s = \begin{bmatrix} 0 & 0 & -1 \end{bmatrix}$$

Stacking $\mathcal{W}_m$ and $\mathcal{W}_s$ yields the constraint Jacobian matrix. Likewise, we find $\boldsymbol{a}$ and $\boldsymbol{\Phi}$. Since $\mathcal{W}$ possesses six independent columns and determinant$(\mathcal{W}^{\mathrm{T}}\mathcal{W}) = 20$, the formula (16) gives the vector of constraint forces, which provides forces that carry out the path maneuvering task and the synchronization task. These forces have to be applied to the vehicles through the actuators.

Due to unactuated sway dynamics, it is impossible to apply the corresponding forces (i.e. the second and the fifth elements of $\boldsymbol{\tau}_c$ denoted by $\tau_{c,2}$ and $\tau_{c,5}$, respectively) to the vehicles. To circumvent the problem, we take the same line of thinking as [22]. The solution is to make $\tau_{c,2}$ and $\tau_{c,5}$ equal to zero by utilizing the unassigned signals $v_{d,m}$ and $v_{d,s}$. Setting $\tau_{c,2}$ and $\tau_{c,5}$ zero yields two differential equations as:

$$\tfrac{1}{2}m_{22,m}\dot{v}_{d,m} = -d_{22,m}v_{d,m} + g_m(\boldsymbol{\zeta}, t) + u_{v_{d,m}}(t) \tag{33a}$$
$$\tfrac{1}{2}m_{22,s}\dot{v}_{d,s} = -d_{22,s}v_{d,s} + g_s(\boldsymbol{\zeta}, t) + u_{v_{d,s}}(t) \tag{33b}$$

in which $\boldsymbol{\zeta} = [\boldsymbol{K}_m^{\mathrm{T}}, \boldsymbol{K}_s^{\mathrm{T}}, \dot{\boldsymbol{G}}_m^{\mathrm{T}}, \dot{\boldsymbol{G}}_s^{\mathrm{T}}, \boldsymbol{G}_m^{\mathrm{T}}, \boldsymbol{G}_s^{\mathrm{T}}]^{\mathrm{T}}$, and $g_j(\boldsymbol{\zeta}, t)$ and $u_{v_{d,j}}(t), j = \{m, s\}$ are found by inspection.

We would like to draw the reader's attention to the fact that the control law derived from this method is based on the least-squares. That is, the control law provides the best forces that make the geometric errors $[\boldsymbol{\varepsilon}_f^{\mathrm{T}}, \boldsymbol{\varepsilon}_{pf}^{\mathrm{T}}]^{\mathrm{T}}$ GES in addition to making $[\boldsymbol{K}_m^{\mathrm{T}}, \boldsymbol{K}_s^{\mathrm{T}}, G_{m,1}, G_{m,2}]^{\mathrm{T}}$ GES. We can easily show that $[G_{m,1}, G_{m,2}]$ is GES. However, to establish uniform global asymptotic stability (UGAS) of $\xi = [\boldsymbol{\varepsilon}_f^{\mathrm{T}}, \boldsymbol{\varepsilon}_{pf}^{\mathrm{T}}, \boldsymbol{K}_m^{\mathrm{T}}, \boldsymbol{K}_s^{\mathrm{T}}]^{\mathrm{T}}$ requires more work. It is viable to show that there exists a $\Delta^* > 0$ such that ξ is UGAS if $\Delta > \Delta^*$.

Remark 4: Notice that the proposed controller is a dynamic controller. In fact, underactuated marine craft possess a second-order nonholonomic constraint [23]. Therefore, in the proposed approach, first-order nonholonomic constraints are treated by the stabilization procedure whereas second-order nonholonomic constraints inject dynamics into the control system.

VI. Simulation Results

A nonlinear model of INFANTE AUV [24] is used for simulating a realistic environment. The INFANTE AUV is unactuated in sway. The contribution of the rudder is seen in both the surge and the sway dynamics. The maximum propeller thrust is $920\,\mathrm{N}$ which makes the AUV move at a speed of $5\,\mathrm{m/s}$ in calm water. The rudder deflection saturates at $30°$. Actuator dynamics is approximated by a first-order transfer function. This system is described by a simplified model according to (20) which is used for designing the controller.

Two identical vehicles are considered. The desired path is described by $\boldsymbol{p}_p(\varrho) = [-60, \varrho]^{\mathrm{T}}$. The initial conditions are $\boldsymbol{q}_{0,m} = [-50, -90, \pi/2]^{\mathrm{T}}, \boldsymbol{q}_{0,s} = [-90, -100, \pi/4]^{\mathrm{T}}$ and $\boldsymbol{\nu}_{0,m} = \boldsymbol{\nu}_{0,s} = [1.5\,\mathrm{m/s}, 0, 0]^{\mathrm{T}}$. The controller gains are selected as $\mathcal{P}_{G,m} = \mathcal{P}_{G,s} = \mathrm{diag}\{1, 1, 1\}, \mathcal{P}_{\Phi,m} = \mathrm{diag}\{30, 20, 1, 1, 1\}$, and $\mathcal{P}_{\Phi,s} = \mathrm{diag}\{5, 2, 1, 1, 1\}$. $\Delta = 20\,\mathrm{m}$ and $u_d = 2.5\,\mathrm{m/s}$.

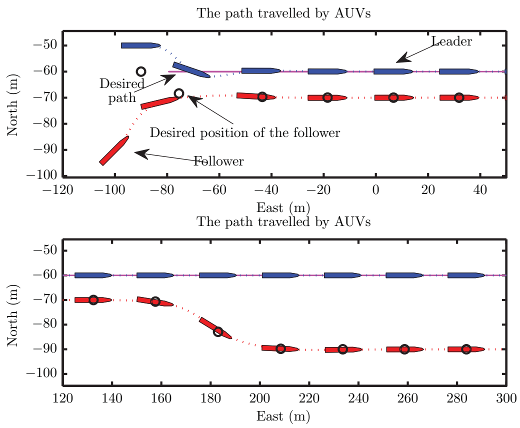

Fig. 3: Formation of two marine craft in calm water. The desired distance changes after $t = 90\,\mathrm{s}$.

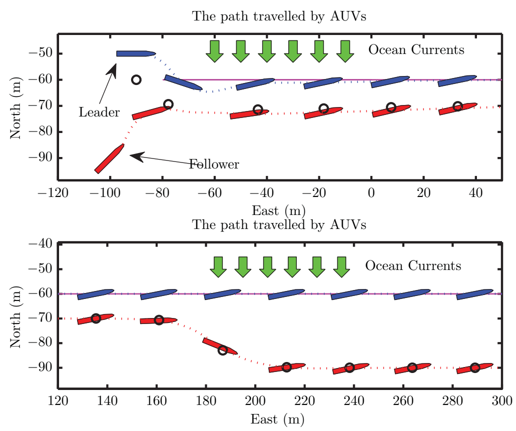

Fig. 4: Formation of two marine craft in the presence of ocean currents. Integral action is augmented to the controller.

The desired formation is given by $\boldsymbol{\varepsilon}_d = [0, -10]^{\mathrm{T}}$ for $t < 90\,\mathrm{s}$. $\boldsymbol{\varepsilon}_d$ smoothly changes to $[0, -20]^{\mathrm{T}}$ for $t \geq 90\,\mathrm{s}$. The examination is performed for two cases.

Ideal Condition: In this case, the simulation is carried out in the absence of external disturbances. Fig. 3 contains two blow-ups of the simulation result.

In the Presence of Ocean Currents: Now, a current with the speed vector $\dot{\boldsymbol{q}}_c = [-.5\,\mathrm{m/s}, 0, 0]^{\mathrm{T}}$ perturbs the craft. To make the controller robust, integral action is augmented to the stabilization procedure. Fig. 4 shows the result of the simulation.

Discussions

Simulation results reveal that the algorithm is successful to accomplish both path maneuvering and synchronization tasks. It is also demonstrated that in the presence of ocean currents, augmentation of integral action can be a remedy for fragility of the control system. Integrators can be placed only for the geometric errors (i.e. $\boldsymbol{\varepsilon}_f$ and $\boldsymbol{\varepsilon}_{pf}$) and there is no need for adding integrators for the constraints on the sway and yaw dynamics. In fact, constant ocean currents force underactuated marine craft to rotate so that a component of the forward velocity is provided in order to counteract the component of ocean currents that is normal to the path; with integral action, this approach makes ψ_r and e zero. On the other hand, if $e = 0$ then $\tilde{\psi} \neq 0$ and $\psi - \psi_p \neq 0$. The reason is that ψ_d is found such that x-axis of $\{b\}$ is aligned along the line of sight.

In this paper, $\boldsymbol{p}^*$ and ψ^* are chosen as $\boldsymbol{p}_m$ and χ_m, respectively. Actually, the path traveled by the leader is approximated with straight-line segments with the slope χ_m at each instant of time. $\chi_m = \psi_m + \beta_m$ is termed as the course angle, which is the angle that the overall speed makes in $\{i\}$, and $\beta_m = \arctan(v_m/u_m)$ is called the sideslip angle.

REFERENCES

[1] R. Ghabcheloo, A. P. Aguiar, A. Pascoal, C. Silvestre, I. Kaminer, and J. Hespanha, "Coordinated path-following control of multiple underactuated autonomous vehicles in the presence of communication failures," in *Decision and Control, 45th IEEE Conf. on*, pp. 4345–4350, 2006.

[2] H. Bai, M. Arcak, and J. Wen, *Cooperative Control Design*. Communications and Control Engineering, Springer, 2011.

[3] K. Pettersen, J. Gravdahl, and H. Nijmeijer, eds., *Group Coordination and Cooperative Control*. Springer, 2006.

[4] V. Kumar, N. Leonard, and A. Morse, eds., *Cooperative Control*. Lecture Notes in Control and Information Sciences, Springer, 2005.

[5] E. Børhaug, A. Pavlov, E. Panteley, and K. Y. Pettersen, "Straight line path following for formations of underactuated marine surface vessels," *Control Sys. Tech., IEEE Trans. on*, vol. PP, no. 99, pp. 1–14, 2010.

[6] F. Fahimi, "Sliding-mode formation control for underactuated surface vessels," *Robotics, IEEE Trans. on*, vol. 23, pp. 617 –622, 2007.

[7] W. Dong and J. Farrell, "Formation control of multiple underactuated surface vessels," *Cont. Theory App., IET*, vol. 2, pp. 1077 –1085, 2008.

[8] P. Encarnacao and A. Pascoal, "Combined trajectory tracking and path following: an application to the coordinated control of autonomous marine craft," in *CDC, IEEE conf.*, vol. 1, pp. 964–969, 2001.

[9] R. Skjetne, S. Moi, and T. Fossen, "Nonlinear formation control of marine craft," in *CDC, IEEE Conf.*, vol. 2, pp. 1699 – 1704, 2002.

[10] F. Arrichiello, S. Chiaverini, and T. I. Fossen, "Formation control of marine surface vessels using the null-space-based behavioral control," in *Group Coordination and Cooperative Control*, Springer, 2006.

[11] I. A. F. Ihle, J. Jouffroy, and T. I. Fossen, "Formation control of marine surface craft: A lagrangian approach," *Oceanic Engineering, IEEE Journal of*, vol. 31, no. 4, pp. 922–934, 2006.

[12] M. O. Miller and J. A. Combs, "The next underway replenishment system," *Naval Engineers Journal*, vol. 111, no. 2, pp. 45–55, 1999.

[13] L. A. Pars, *A Treatise on Analytical Dynamics*, 1965.

[14] B. Siciliano, L. Sciavicco, L. Villani, and G. Oriolo, "Mobile robots," in *Robotics*, pp. 469–521, Springer, 2009.

[15] C. Lanczos, *The variational principles of mechanics*. 4^{th} ed., 1986.

[16] M. R. Flannery, "The enigma of nonholonomic constraints," *American Journal of Physics*, vol. 73, no. 3, pp. 265–272, 2005.

[17] M. Krstic, P. Kokotovic, and I. Kanellakopoulos, *Nonlinear and adaptive control design*. John Wiley & Sons, 1995.

[18] J. Slotine and W. Li, *Applied nonlinear control*. Prentice Hall Englewood Cliffs, 1991.

[19] T. I. Fossen, *Handbook of marine craft, hydrodynamics, and motion control*. John Wiley & Sons Ltd., 2011.

[20] R. Skjetne, T. I. Fossen, and P. V. Kokotovic, "Adaptive maneuvering, with experiments, for a model ship in a marine control laboratory," *Automatica*, vol. 41, no. 2, pp. 289–298, 2005.

[21] M. Breivik and T. I. Fossen, "Guidance laws for autonomous underwater vehicles," in *Underwater Vehicles* (A. V. Inzartsev, ed.), InTech, 2009.

[22] E. Peymani and T. I. Fossen, "A lagrangian framework to incorporate positional and velocity constraints to achieve path-following control," in *CDC-ECC, IEEE Conf.*, pp. 3940 –3945, 2011.

[23] K. Wichlund, O. Srdalen, and O. Egeland, "Control of vehicles with second-order nonholonomic constraints: Underactuated vehicles," in *ECC*, 1995.

[24] C. J. F. Silvestre, *Multi-objective optimization theory with applications to the integrated design of controllers/plants for autonomous vehicles*. PhD thesis, Dep. of Elec. Eng., Instituto Superior Tecnico (ISR), 2000.